First principles investigations on the electronic structure of anchor groups on ZnO nanowires and surfaces

A. Dominguez, M. Lorke, A. L. Schoenhalz, A. L. Rosa, Th. Frauenheim, A. R. Rocha, and G. M. Dalpian

Citation: Journal of Applied Physics **115**, 203720 (2014); doi: 10.1063/1.4879676
View online: http://dx.doi.org/10.1063/1.4879676
View Table of Contents: http://scitation.aip.org/content/aip/journal/jap/115/20?ver=pdfcov
Published by the AIP Publishing

First principles investigations on the electronic structure of anchor groups on ZnO nanowires and surfaces

A. Dominguez,[1,a)] M. Lorke,[1,a)] A. L. Schoenhalz,[2,a)] A. L. Rosa,[1] Th. Frauenheim,[1] A. R. Rocha,[3] and G. M. Dalpian[2]
[1]*BCCMS, Universität Bremen, Am Fallturm 1, 28359 Bremen, Germany*
[2]*CCNH, Universidade Federal do ABC, Av. dos Estados 5001, Santo André, Brazil*
[3]*IFT, Universidade Estadual Paulista, R. Dr. Bento Teobaldo Ferraz, 271, São Paulo, Brazil*

(Received 3 March 2014; accepted 13 May 2014; published online 30 May 2014)

We report on density functional theory investigations of the electronic properties of monofunctional ligands adsorbed on ZnO-(10$\bar{1}$0) surfaces and ZnO nanowires using semi-local and hybrid exchange-correlation functionals. We consider three anchor groups, namely thiol, amino, and carboxyl groups. Our results indicate that neither the carboxyl nor the amino group modify the transport and conductivity properties of ZnO. In contrast, the modification of the ZnO surface and nanostructure with thiol leads to insertion of molecular states in the band gap, thus suggesting that functionalization with this moiety may customize the optical properties of ZnO nanomaterials. © *2014 AIP Publishing LLC*. [http://dx.doi.org/10.1063/1.4879676]

I. INTRODUCTION

The combination of organic and inorganic materials for the fabrication of devices with novel properties has received considerable attention in technology. In particular, devices based on nanostructured materials are highly sensitive to adsorbed compounds due to their large surface-to-volume ratios. ZnO is an important candidate for the assembly of such devices, partly because of the possibility of fabrication of a large number of ZnO nanostructures.[1] Adsorption of molecular layers can modify the properties of ZnO surfaces and provide a strategy for further immobilization of dyes and biomolecules. It has been reported that the electrical and optoelectronic performance of ZnO nanobelts are improved via functionalization with carboxylic acids.[2] The enhancement in conductivity was attributed to the passivation of the nanobelt surface, which prevents that the oxygen in the surrounding environment reacts with point vacancies at the surface. Recently, it has been demonstrated that adsorbates can also assist charge separation and suppression of back recombination in nanostructured ZnO/P3HT interfaces.[3]

Several molecules have been investigated to determine the most appropriate anchor groups for the functionalization of ZnO. Compounds that has been employed as ligands include carboxylic acids,[4–12] amines,[13–15] silanes,[4,16–18] phosphonic acids,[19] and thiols.[14,19–22] Aside from a required covalent binding between the anchor group and the substrate, the electronic structure of the adduct determines the suitability of the ligand for a desired function of the modified nanostructure. In ZnO nanoparticles, for instance, the presence of molecular states in the energy gap may affect the emission efficiency in ZnO-based ultraviolet (UV) lasers. However, this can be a desired feature for detection of water contaminants in photocatalytic sensors.[23]

Fourier-transform infrared (FT-IR) and UV spectroscopy indicated that carboxylic acids are promising anchor groups for ZnO. However, it appears that the amount, adsorption position, and acidity of these ligands as well as the solution pH should also play a role in the binding properties.[24] On the other hand, recent atomic force microscopy (AFM) measurements have refuted the rightness of carboxylic acids for the modification of ZnO, showing that alkyl carboxylic acids etch the surface.[25] Thiols have also been suggested to form strong bonds on ZnO.[16,26] Alkanethiols were found to bind to the surface, forming highly uniform monolayers with some etching detected after long immersion times in an alkanethiol solution.[25] However, earlier investigations reported non-uniform coverages or even physisorbed layers of these functional groups.[24]

Several chemisorbed[27–31] and physisorbed molecules[32–37] on ZnO have been theoretically investigated. The chemical stability of carboxyl (-COOH) groups on ZnO has been confirmed by theoretical tight-binding[27] and first-principles calculations.[28,29] A combined investigation using first-principles and FT-IR experiments concluded that molecules containing acetylacetone are as good anchors as carboxylic acid on ZnO (10$\bar{1}$0).[28,30] In a previous work, we showed that -COOH, thiol (-SH), amino (-NH_2),[27,29,38] and phosphonic acid ($PO(OH)_2$)[39] groups chemisorb onto the ZnO (10$\bar{1}$0) surfaces with binding energies typically within 1–3 eV.

In most theoretical works on ZnO functionalization thus far, the generalized-gradient approximation (GGA) within the Perdew-Burke-Ernzerhof (PBE) formalism[40,41] has been employed for the study of the structural and electronic properties of the modified systems. Whereas geometries are reliably given within this approach, electronic structures suffer from the well known band-gap problem of semi-local density functionals. In the case of ZnO, this error is striking as GGA yields a band gap of 0.7 eV, which highly underestimate the experimental value of 3.4 eV. One of the reasons for this underestimation is given by the wrong description of the

[a)]A. Dominguez, M. Lorke, and A. L. Schoenhalz contributed equally to this work.

location of Zn-3*d* states, which lie around 2 eV higher in energy compared to experiment.[42] Accurate many-body techniques such as GW are found to correct the band gap and the position of Zn-3*d* states in bulk ZnO.[43] However, its applicability to more complex systems such as surfaces and interfaces is still cumbersome. Hybrid density functional approaches, where a fraction of Hartree-Fock exchange is admixed, improves upon physical and chemical properties of solids and molecules. In general, the description of bond lengths, ionization energies, cohesive properties, and band gaps are in much better agreement with experiment when employing hybrid functionals.[44] In this work, we use PBE0,[45,46] to investigate the electronic properties of ZnO/organic interfaces. We employ substituted methane molecules of the type CH_3-X with X = -COOH, -SH, and -NH_2 as prototype adsorbates. In Sec. II, the computational details of our calculations are described. In Sec. III A, we report on the electronic structure of the ZnO $(10\bar{1}0)$ surface modified with the aforementioned moieties. The nonpolar $(10\bar{1}0)$ is the most stable surface of ZnO and is the majority facet in many grown ZnO nanostructures.[1] Afterwards, in Sect. III B we address the adsorption of the anchor groups on the nonpolar facets of an ultrathin ZnO nanowire. The analysis of the electronic structure was done using the averaged electrostatic potential between the bulk and the surfaces, and the vacuum level between the surfaces and the wires. We show that neither the valence band maximum (VBM) nor the conduction band minimum (CBM) of the bare surface shift significantly compared to the bulk value. This allowed us to use the vacuum level of the bare surface as a reference to align the energy levels of the surface with those of the ligands. We find that the molecular state follows the band gap opening for nanostructures, instead of being pinned to a specific energetic range.

II. COMPUTATIONAL DETAILS

Periodic density functional theory (DFT) calculations were performed as implemented in the Vienna *ab-initio* Simulation Package (VASP).[47–50] Plane wave basis functions with an energy cutoff of 400 eV and 300 eV have been employed for the surface and nanowire systems, respectively. The projector-augmented wave (PAW) method[51,52] has been used throughout. The geometries were optimized at the PBE level. The electronic structures for the optimized geometries were calculated within the hybrid PBE0 formalism. For the Brillouin zone integration, we employed Monkhorst-Pack (MP)[53,54] meshes of $(4 \times 4 \times 4)$ for bulk, $(1 \times 4 \times 4)$ for the surfaces, and $(1 \times 1 \times 4)$ for the nanowires (NWs). For the calculation of the density of states (DOS), MP grids of $(1 \times 10 \times 10)$ for the surfaces and $(1 \times 1 \times 10)$ for the NWs were used. All atomic positions have been relaxed until the interatomic forces were smaller than 0.01 eV/Å.

III. RESULTS

A. Surfaces

The use of PBE0 substantially improves upon the band gap of bulk ZnO, yielding a value of 3.2 eV, which is much more in line with the experimental value.[55] To uniquely compare our PBE and PBE0 results for bulk ZnO, we employ the method proposed in Ref. 56, where the band edges of the solid are aligned using the electrostatic potential averaged along the y-z plane, resulting from the PBE and PBE0 calculations. We find that for bulk ZnO the VBM as obtained with PBE0 is shifted downwards by 1.6 eV with respect to the PBE value, in very good agreement with the results reported in Ref. 57. The Zn 3*d* states have a binding energy of 7.5 eV. The CBM, mainly composed of Zn-4*s* states, shifts upwards by 0.7 eV within PBE0, compared to the PBE results.

To model the bare surface, we consider a tetragonal supercell consisting of a wurzite ZnO slab containing 8 Zn-O atomic layers and a vacuum region of approximately 17 Å along the $[10\bar{1}0]$ direction. For the modified surfaces, the same supercell dimensions were employed. The corresponding optimized structures are depicted in Fig. 1. Two molecules per supercell (one at each side of the slab) with equivalent configurations were considered. This leads to one ligand per surface unit cell. As we have shown in previous studies,[27,29,58] this surface coverage is the thermodynamically most stable one.

Our results show that both -COOH and -SH groups adsorb on the surface in a dissociative manner, while -NH_2 does not dissociate (see Fig. 1). This fact plays an important role in the resulting electronic structure as will be discussed in what follows. The adsorption energies, which provide information about how the surface and the molecules interact, are calculated as $E_{ads} = \frac{1}{n}(E_T - E_{Bare} - E_{mol})$, where E_T is the total energy of the hybrid system (surface + molecule), E_{Bare} is the total energy of bare surface, n is the number of molecules adsorbed on the surface, and E_{mol} is the energy of a neutral (isolated) molecule in gas phase. Using the PBE0 functional, the obtained adsorption energies are −1.35 eV, −0.76 eV, and −0.90 eV, for -COOH, -NH_2, and -SH cases, respectively. These energies compare well to previously obtained values at the PBE level (−1.39 eV, −0.88 eV, and −1.03 eV for -COOH, -NH_2, and -SH, respectively.[29])

The distributions of the optimized atomic bond distances as obtained with either PBE or PBE0 are shown in Fig. 2. We can conclude that there are no significant changes between PBE0 and PBE results, thus demonstrating that the

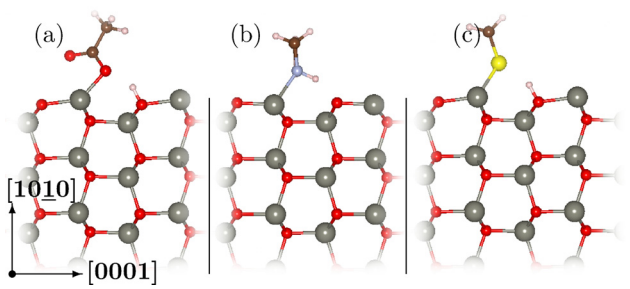

FIG. 1. Optimized structures of the ZnO $(10\bar{1}0)$ surface covered with one monolayer of (a) CH_3-COOH, (b) CH_3-NH_2, and (c) CH_3-SH molecules. The spheres represent the following atoms with the corresponding color within parenthesis: oxygen (red), zinc (gray), carbon (brown), nitrogen (light blue), sulfur (yellow), and hydrogen (light pink).

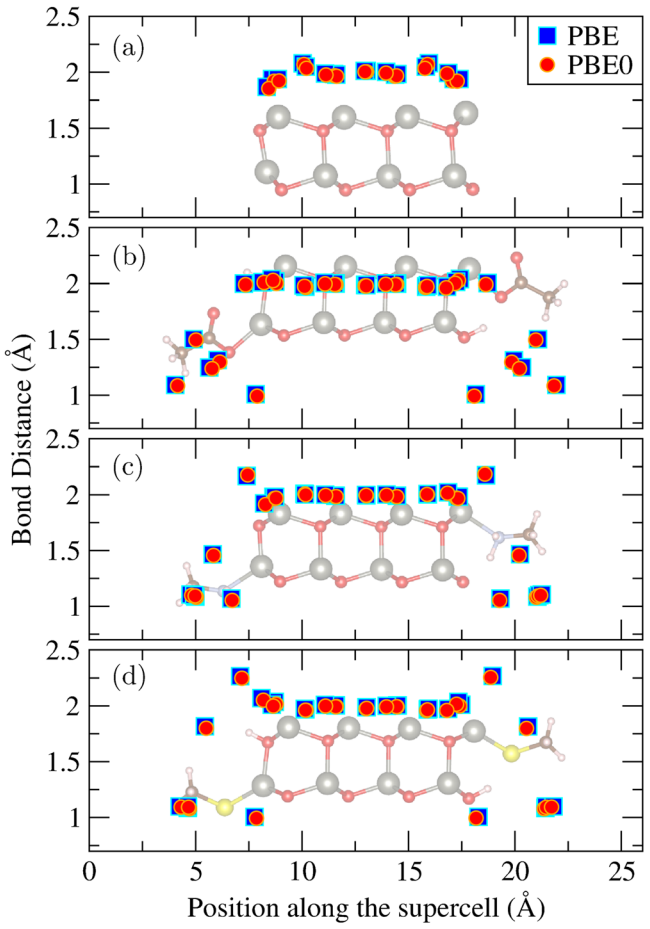

FIG. 2. Bond lengths for (a) the bare and modified ZnO surfaces using (b) CH_3-COOH, (c) CH_3-NH_2, and (d) CH_3-SH ligands obtained at the PBE and PBE0 levels of theory.

latter functional provides an accurate structural description for these systems. In the center of the slab, all systems feature Zn-O interatomic distances similar to those found for bulk ZnO (around 2.0 Å). The main difference in bond lengths can be observed at the surface, where the bond distances are longer than for bulk for the -COOH and -SH cases, whereas they are shorter for the bare and -NH_2-modified surfaces. The latter two cases are the ones with the presence of dangling bonds at the surface (dangling bonds at the oxygen binding sites are passivated for -COOH and -SH due to dissociation of the ligands).

The alignment of the energy levels shows that the VBM of the bare surface does not shift significantly (see Appendix) compared to the bulk value. Subsequently, the band alignment has been done using the vacuum level of the bare surface and the adsorbed systems as in Refs. 59–62. We have ensured that the vacuum region of the supercell is large enough, so that the electrostatic potential reaches its vacuum value and is flattened out.

Fig. 3 shows the total and projected DOS for the bare surface and surfaces with adsorbed molecules using the band alignment described above. The DOS are aligned in such way that the zero on the *x*-axis corresponds to the VBM for the bare surface. The band structures for the bare and modified surfaces are presented in Fig. 4. The band alignment corresponds to that employed for the DOS. The calculated band gap of the bare surface in this work is ∼3.15 eV. Here, quantum confinement effects due to reduction of the dimensionality are counteracted by the presence of surface levels

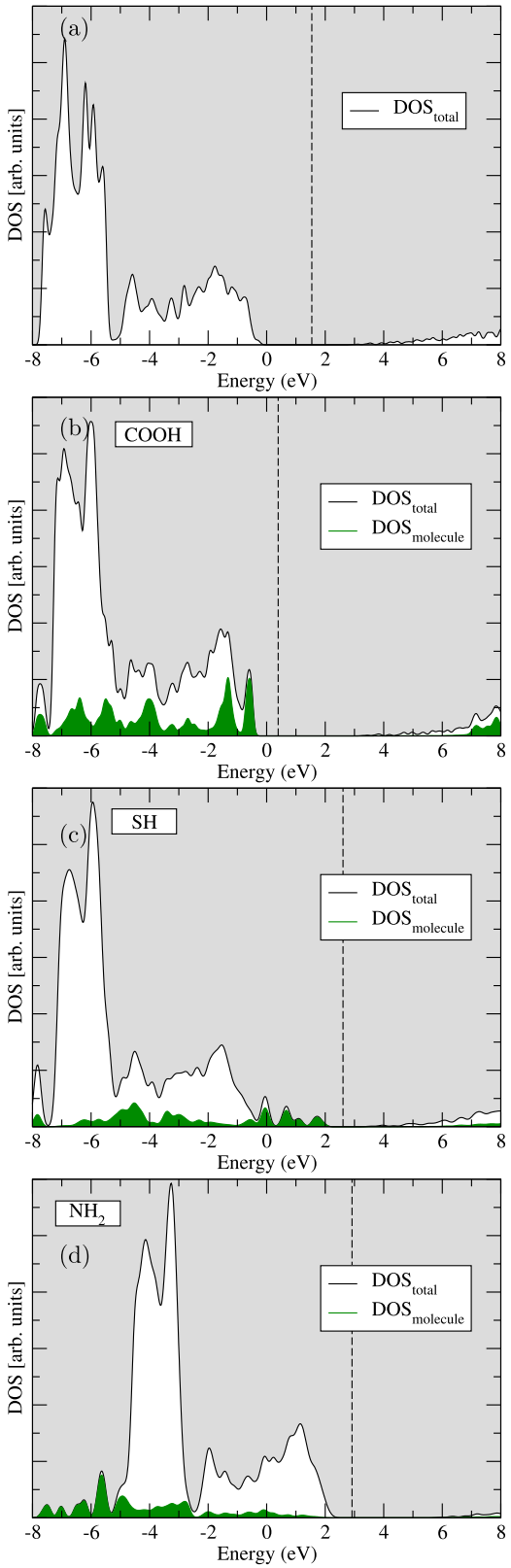

FIG. 3. Projected DOS for (a) the bare and modified surfaces with (b)-COOH, (c)-SH, and (d)-NH_2 groups. The black and green lines represent, respectively, the total DOS and its projection onto the ligand states. The dashed line denotes the Fermi energy.

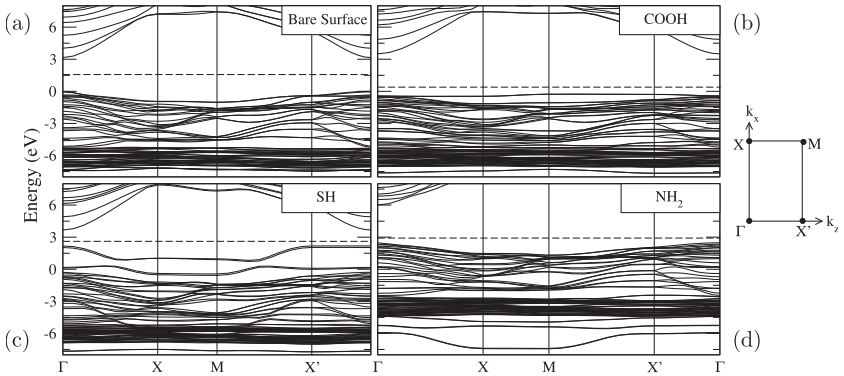

FIG. 4. Band structure for the bare surface (a) and the surface with adsorbed molecules: -COOH (b), -SH (c), and -NH_2 (d). The picture on the right side represents the path sampling in the Brillouin zone.

(dangling bonds) resulting in a band gap only slightly larger than that of bulk ZnO (~3.09 eV). From Figs. 3 and 4, we can observe that only in the case of modification with -SH, molecular levels are inserted in the band gap. In contrast, -COOH molecular levels contribute to the valence band edge due to hybridization of states of the carboxyl oxygen and the substrate. For the -NH_2 case, occupied molecular levels are located deeper in the valence band.

B. Nanowires

We now investigate the effects of the change in dimensionality on the electronic properties of organic-ZnO interfaces by considering the same adsorbates on thin ZnO NWs. The NWs have been modeled using infinitely long ZnO wires with hexagonal cross sections, grown along the [0001] direction. The bare NW exhibits nonpolar $(10\underline{1}0)$ and $(1\underline{2}10)$ facets as shown in Fig. 5. We consider a supercell containing 48 atoms[63] and a sufficiently large vacuum region in order to avoid spurious interactions with the supercell images. For the modified NWs a monolayer (ML) of ligands (one ligand per surface Zn-O pair) was considered. This amounts to 12 molecules per supercell. We have shown in a previous investigation that a monolayer coverage is energetically favored over lower coverages for the modification of ZnO surfaces.[29] We chose alternate orientation of the molecules in such a way that on the $(10\underline{1}0)$ facet the ligands point to the same direction whereas the orientation is exchanged in neighboring $(10\underline{1}0)$ facets (see Fig. 5).

We first investigate the bare NW. To test the reliability of the PBE functional for the description of the investigated structure, we performed a geometry optimization calculation using the PBE0 functional. The optimized geometry at the PBE0 level of theory is shown in Fig. 5. Both O and Zn atoms of the surface layer relax towards the bulk region. However, the relaxation for Zn is larger than for O atoms, thus leading to formation of a buckled surface Zn-O dimer. This relaxation shrinks the surface Zn-O bond length from the bulk value (2.01 Å) to 1.88 Å. The distance between nearest neighbor Zn atoms along the wire growth direction varies from 3.2 Å in the bulk region to 3.0 Å close to the surface. The tilt angles of the surface Zn-O dimer are $\omega_1 = 10.4^\circ$ and $\omega_2 = 3.7^\circ$, respectively, according to the definitions used in Ref. 63. The good agreement between these results and earlier PBE findings,[63] together with the experience gained from the surface calculations, give us confidence to select the PBE functional for the structural relaxation of the modified NWs.

In Figs. 6(a) and 9(a), the projected DOS and the band structures along the Γ-A direction are shown for the bare NW. The energy levels of the different structures have been aligned using the electrostatic potential of the vacuum region as in Refs. 59–62, setting the VBM of the bare surface as zero of the energy scale in all cases.

The system has a direct band gap of 3.7 eV at the Γ-point. The increase of the band gap compared to the bulk case is due to quantum confinement effects on the band edges. As expected from a simple particle-in-a-box-like picture, the CBM is more affected by quantum confinement than the VBM, due to the difference in effective masses of electrons at the CBM and holes at the VBM. From the projected DOS, we can infer that the VBM is composed of O_A-*p* states, shifted 0.1 eV from the bulk-like O_C-p states (data not shown). In contrast, the CBM is made of Zn_C-s states belonging to the bulk region of the NW. Compared to bulk ZnO, Zn-*d* and O-*p* states have a stronger overlap. The effective masses for the highest valence band and lowest conduction band are $-0.048\,m_e$ and $0.008\,m_e$, respectively, where m_e is the electron mass.

Next, we discuss on the modified ZnO NWs. The optimized structure for the -COOH-covered wire is shown in Fig. 7. The -COOH group adsorbs via two asymmetric bonds between the carboxyl oxygens, O_1 and O_2, and the surface Zn atoms. This is accompanied by a proton transfer from the anchor group to the surface O_A atom. The intra-molecular angle O_1-C-O_2 of the moiety is 120°. After adsorption of the ligand, the surface Zn-O bond length is nearly restored to its bulk value (2.05 Å). Similarly, the distance between nearest neighbors Zn atoms along the wire axis is reduced to 3.1 Å.

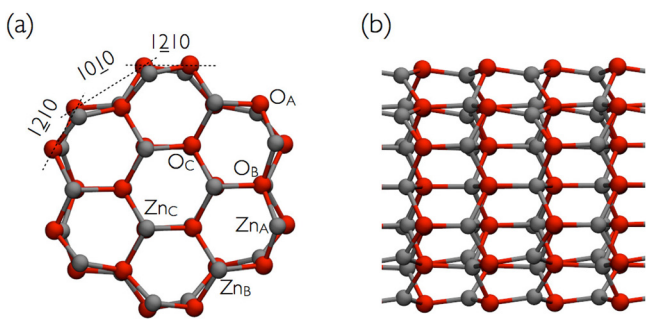

FIG. 5. Optimized structure of the bare NW: (a) top view and (b) side view.

Our findings agree with Fourier transform infrared attenuated total reflectance measurements on ZnO nano tips functionalized with carboxylic acid, which show a loss of the carbonyl bond (C = O). This is in line with a bidentate attachment of the -COOH group on the surface as found in our calculations.

The DOS and electronic structure for the -COOH-ZnO system are shown in Figs. 6(b) and 9(b), respectively. We find strong changes in the band structure around the VBM. Specifically, the surface O_A *p*-states hybridize with O_1 and O_2 *p*-states of the functional group, resulting in localized states at −0.5 eV. The electronic structure reveals that the band gap becomes indirect, as the localized states have a slight dispersion to higher energies at the A-point. This resembles the behavior for the adsorption on the surface, where also an indirect gap is found (see Fig. 4). In general terms, the electronic structures for the -COOH-modified surface and NW are similar. As for the bare NW, the *p*-states of the O_A atoms have a strong hybridization with Zn-*d* states in the valence band. From the comparison of the DOS projected onto O_A and O_B atoms we can infer that the band bending is significantly reduced to about 0.05 eV, leading to almost flat-band conditions. C-*p* states are mainly located deep in the VB and overlap strongly with the Zn-*d* states. The CBM remains composed of Zn *s*-states of the bulk region. The band gap of the modified wire increases to 4.1 eV. Such modifications of the band gap with respect to the bare nanostructure have been observed for dye-functionalized TiO_2 (Ref. 60) and Si NWs (Ref. 64). They appear due to the interaction between the ligand LUMO and the CBM of the substrate for the former and between the ligand HOMO and the VBM for the latter. Previous GGA + U investigations have already indicated that ZnO $(10\underline{1}0)$ surfaces modified with acetic acid do not feature band gap states. However, for other carboxylic acids, such as benzoic acid, intragap states are observed. The states of the -COOH group are rather localized and should not change the electron mobility in ZnO wires. On the contrary, the hybridization at the VBM even reduces the curvature at the Γ-point, enhancing the hole mobility. Our results confirm the experimental evidences of Ref. 65, where the saturation electron mobility in ZnO thin film FETs functionalized with stearic acid ($CH_3(CH_2)_{16}COOH$) was enhanced by about one order of magnitude. We found that the band bending and curvature of the -COOH-ZnO wire at the Γ-point are reduced compared to the bare NW.

We now turn to the modification of the NW with -SH. The optimized structure is shown in Fig. 8. The most striking difference from the previous cases is the asymmetry between the different adsorbates. Namely, the moieties containing the C_1 and C_3 atoms relax towards each other, while the ones with C_2 and C_4 atoms repel each other. The -SH groups attach to the NW via monodentate S-Zn bonds with a bond length of 2.23 Å for S_2 and 2.26 Å for S_1. The Zn-S-C angle is 106° for the ligands with C_1 and C_3 and 108° for the ligands with C_2 and C_4. Again, the hydrogen atom of the -SH group is transferred to the surface O_A atoms. The NW geometry relaxes significantly with a Zn-O bond length of 2.17 Å. AFM, FT-IR, and X-ray photoelectron spectroscopy (XPS) measurements have indicated a strong S-Zn covalent bond in thiol-functionalized ZnO $(10\underline{1}0)$ surfaces. Moreover, thiol adsorption has also been found experimentally on polar (0001) ZnO surfaces[22] and confirmed via XPS and Raman spectroscopy on ZnO NWs.[22]

The DOS and electronic structure for the -SH-ZnO NW are shown in Figs. 6(c) and 9(c), respectively. Compared to

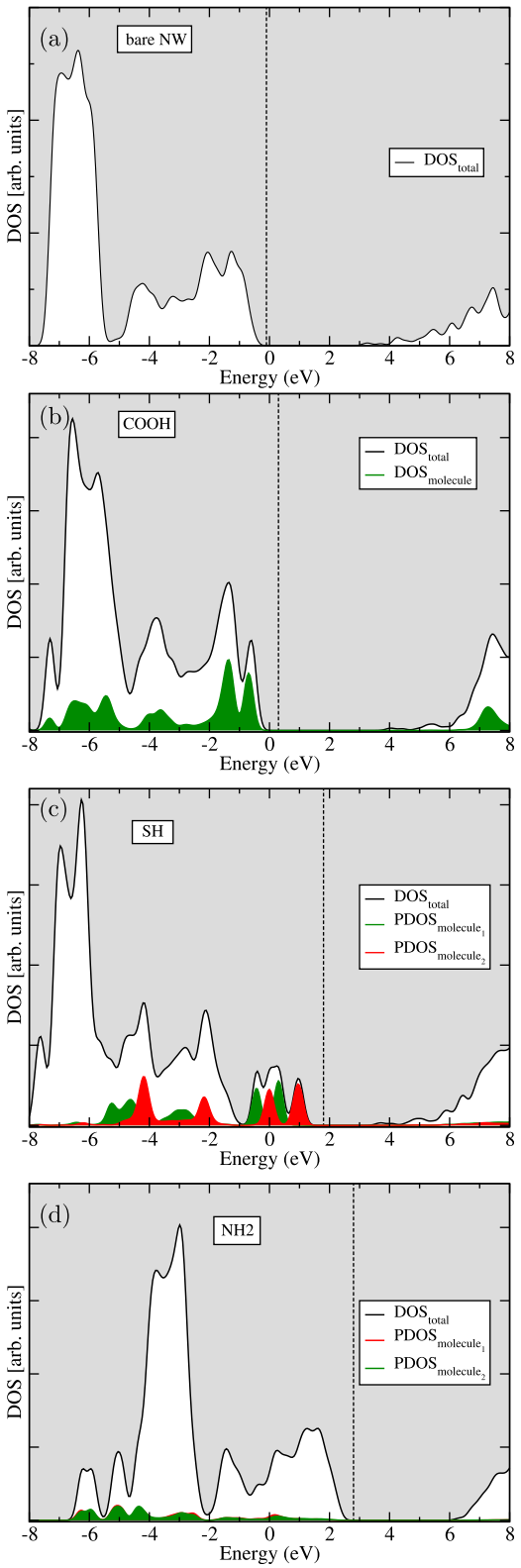

FIG. 6. Projected DOS for (a) the bare and modified NWs with (b)-COOH, (c)-SH, and (d)-NH_2 groups. The dashed line denotes the Fermi energy.

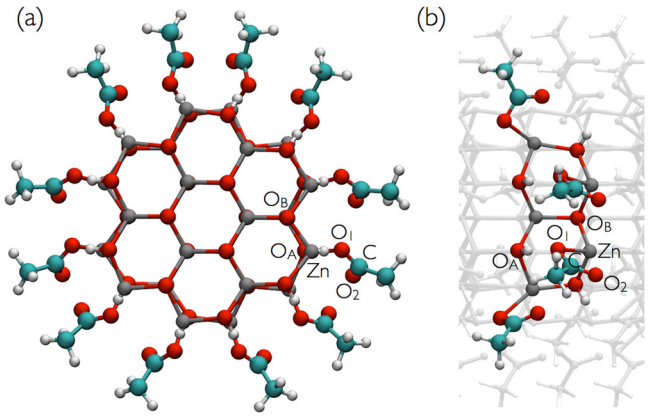

FIG. 7. Optimized structure for the -COOH-modified NW: (a) top view and (b) side view.

the modification with -COOH, the electronic structure undergoes more significant changes. Two molecular states per adsorbate appear in the gap region. These states can be grouped into two subsets. The first one, located energetically at −0.3 eV and 0.7 eV has contributions mainly from the *p*-states of S_1 and C_1, while the second group at 0.5 eV and 1.0 eV stems from the *p*-states of S_2 and C_2. This distinction can be traced back to geometry differences between the two non-equivalent ligands configurations with indexes 1 and 2. The Zn-S_1 and Zn-S_2 bond lengths are different. Also, the distance between C_3 and C_1 is smaller than both C_1-C_2 and C_2-C_4 distances, thus changing the strength of the inter-molecular interaction for the two configurations. The band structure in Fig. 9(c) reveals that the intra-gap states are substantially more localized compared to the surface case (see Fig. 4).

Additionally, we find localized states stemming from the carbon atoms around −4 eV. In contrast to -COOH, the molecular states of the thiol group do not hybridize with the VBM states. In general, it can be stated that the electronic properties of the SH-modified NW are very similar to those for the surface case. Obviously, nondegenerate molecular states due to the two different ligand configurations on the wire are not observed in the surface case, where all adsorbate geometries are equivalent by translational symmetry.

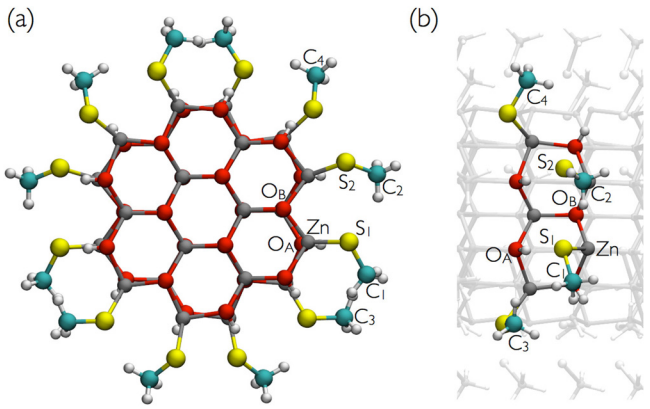

FIG. 8. Optimized structure of the SH-modified NW: (a) top view and (b) side view.

Finally, we investigate the adsorption of the -NH_2 group on the ZnO NW. The corresponding optimized structure is shown in Fig. 10. Similar to the case of -SH group, for the -NH_2-ZnO system we have two nonequivalent ligand dimer configurations. Adsorbates with carbon atoms C_1 and C_3 relax towards each other while those with C_2 and C_4 atoms bend away from each other. The ligands bind to the NW via a monodentate mode with Zn-N_1 and Zn-N_2 bond lengths of 2.15 Å and 2.23 Å, respectively. The Zn-N-C angle is 122° for the ligands with indices 1 and 3 and 136° for those with indexes 2 and 4. Unlike the functional groups investigated so far, -NH_2 does not undergo dissociative adsorption on the wire. A molecular adsorption has been shown to be favorable over ligand dissociation on ZnO nonpolar surfaces in Ref. 29. As an outcome of this binding mode, Zn-O bond lengths relax to about 1.97 Å at the NW surface. The chemisorption

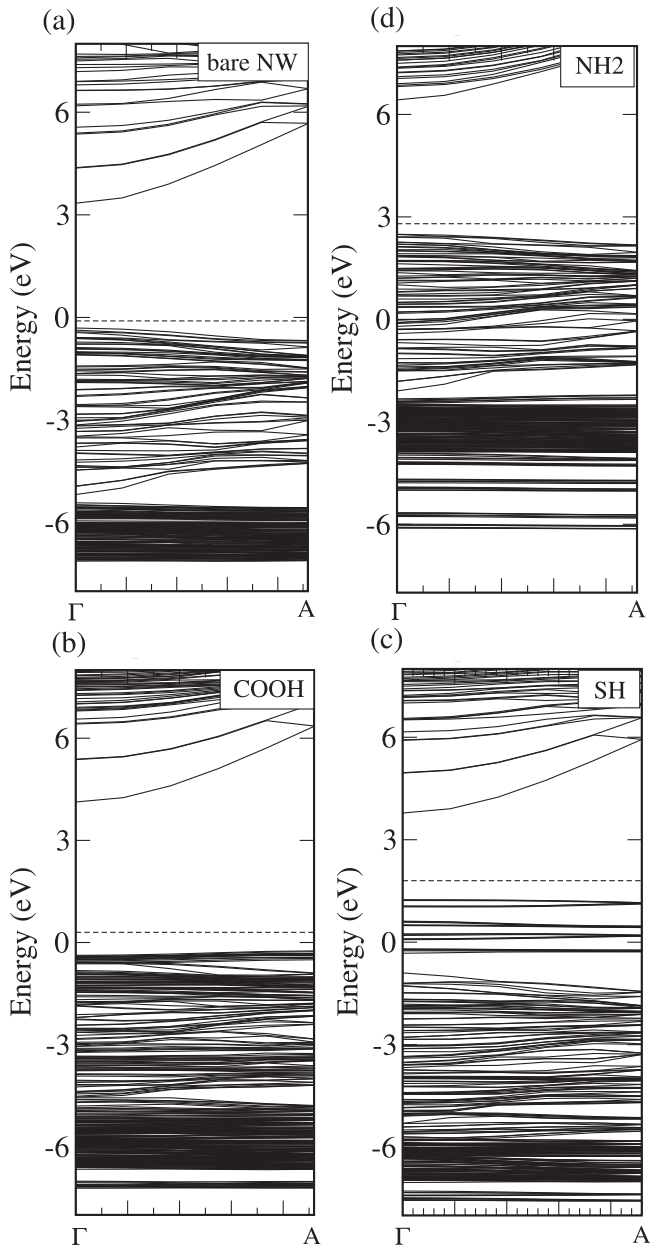

FIG. 9. Band structure along the Γ-A direction for the bare NW (top left) and the NWs modified with -COOH (bottom left), -NH_2 (top right) and -SH (bottom right) groups. The dashed line denotes the Fermi energy.

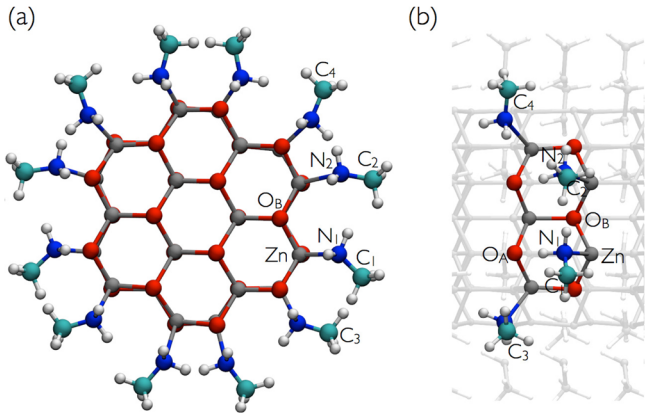

FIG. 10. Optimized structure of the NH_2-modified NW: (a) top view and (b) side view.

of amines on ZnO films has been confirmed by XPS[66] and AFM measurements.

The DOS and band structure for the -NH_2-ZnO system are shown in Figs. 6(d) and 9(d), respectively. Our calculations show that no intra-gap states exist for this system. The VBM is mainly composed of O_A and O_B p-states. The DOS shows a N-*p* component along the entire VB whereas the projection onto the C-*p* states indicates localization in the same energy range as for the Zn-*d* states (data not shown). In contrast to the case of -SH, we find only insignificant differences in the DOS projected on the two nonequivalent groups of adsorbates (see Fig. 6). The most striking feature of the band structure is the large overall shift to higher energies. This behavior is also seen for the -NH_2-modified surface (Fig. 4). This could be explained by noticing that the surface oxygen atoms are non-saturated and the required energy to remove an electron from the dangling bond is therefore reduced compared to the cases where the molecule binds in a dissociative manner. The main feature of the -NH_2-ZnO system is hence a surface passivation that leads to almost perfect flat band conditions in conjunction with a reduced work function.

IV. CONCLUSIONS

We have investigated the electronic properties of ZnO surfaces and NWs modified by several functional groups. We found that the behavior of the investigated moieties is very similar on both surfaces and NWs. Our results suggest that functionalization with carboxylic acids or amines does not alter the transport and conductivity properties of ZnO nanostructures due to the presence of almost flat band conditions. In contrast, the functionalization with thiols might offer a route for modification of optical properties of ZnO nanomaterials due to the appearance of molecular states in the energy gap. Our results provide new insights to improve the physical properties of oxide nanostructures and surfaces for device applications.

ACKNOWLEDGMENTS

We acknowledge financial support from the Deutsche Forschungsgemeinschaft under the program FOR1616, the University of Bremen, and the CAPES/DAAD/PROBRAL international partnership program. We also thank computational resources from HLRN (Hannover/Berlin-Germany) and CENAPAD (São Paulo-Brazil).

APPENDIX: ALIGNMENTS

The alignment between ZnO bulk and surface is presented in Fig. 11. Fig. 12 shows the band alignment for the surface with different functional groups. We can conclude there is again a different trend for the non-dissociated case (-NH_2): the energy difference from vacuum level of bare surface and with adsorbed molecule, defined as the Δ parameter, is positive (∼0.3 eV). For the surface with dissociated adsorbed molecules (-COOH and -SH cases), the Δ has negative values around −1.3 eV.

In case of nano wires, the alignment of the band edges for adsorbed -COOH is shown in Fig. 13. As discussed before, the band edge alignment has been performed with respect to the electrostatic potential in the vacuum region. We find that the surface modification in NWs shifts the CBM upwards in energy by 0.4 eV, while the VBM remains almost unchanged and only the band bending is reduced. This means the beneficial properties of ZnO are preserved, while the surface is stabilized by the functional group. Compared to the isolated molecule, we noted that the surface modification shifts the HOMO of the CH_3-COOH molecule about 0.7 eV upwards and the LUMO upwards by 0.3 eV.

In Fig. 14, the band edge alignment for SH modification of the NW is shown. Now the HOMO of the isolated molecule lies above the VBM of the bare wire. This already indicates a qualitative difference to other functional groups that

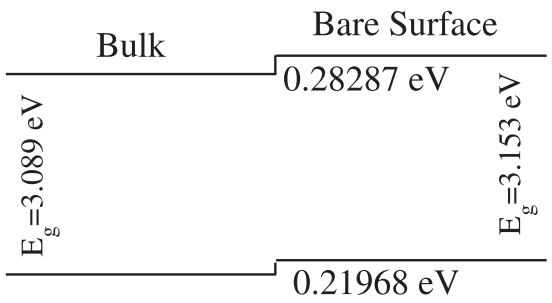

FIG. 11. Band alignment scheme for the studied hybrid interfaces using the vacuum level of the bare surface as the common level.

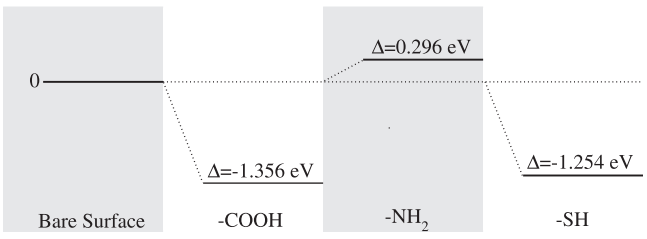

FIG. 12. Band alignment scheme for the studied hybrid interfaces using the vacuum level of the bare surface as the common level.

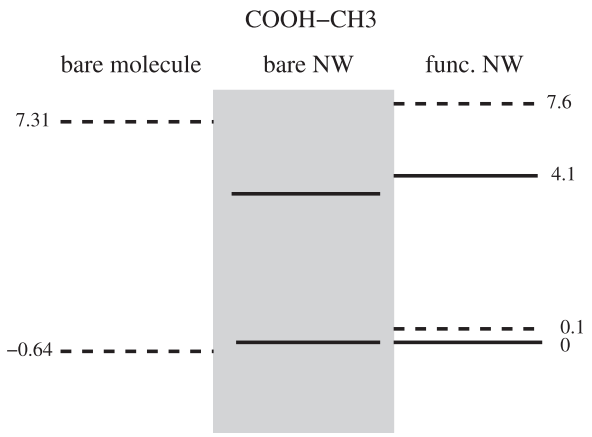

FIG. 13. Band edges alignment for COOH-CH_3 modified ZnO NWs.

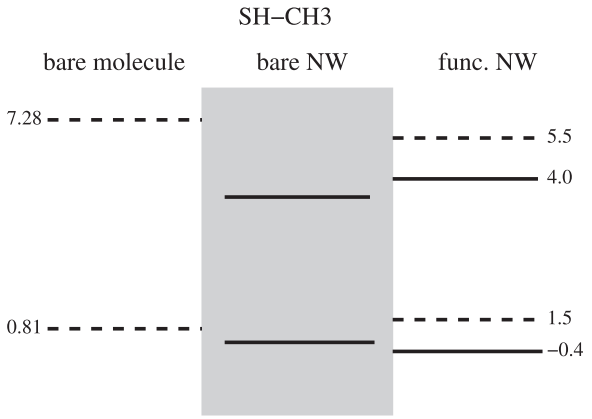

FIG. 14. Band edge alignments for SH-CH_3 modified ZnO NWs.

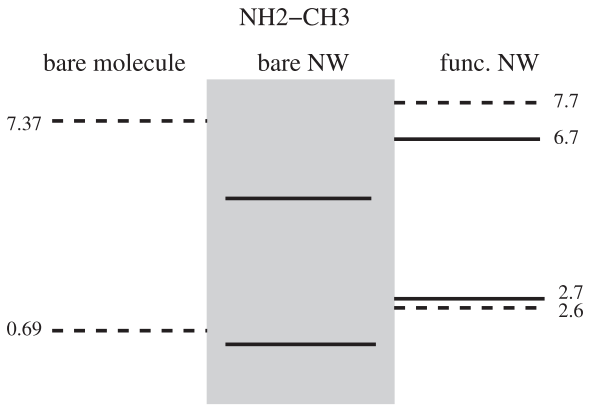

FIG. 15. Band edge alignments for CH_3-NH_2 modified ZnO NWs.

is also reflected in the resulting band structure. In the modified NW, the HOMO of the molecule is shifted up by 0.5 eV while the VBM is shifted downwards by 0.4 eV with respect to the bare NW. The CBM is shifted up by 0.3 eV.

In Fig. 15, the band edges alignment in shown for the CH_3-NH_2 modified NW. We find a pronounced upward shift of all states. The CBM and VBM shift upwards by 2.7 eV and 3.0 eV, respectively, resulting in a band gap of 4 eV. The HOMO states of the molecular groups also shift upwards by 2.9 eV. The reason for this different behavior is probably due to the stronger hybridization of the N-*p* states with all VB states.

[1]Z. L. Wang, *ZnO Bulk, Thin Films and Nanostructures* (Elsevier, Oxford, 2006).
[2]C. Lao, Y. Li, C. P. Wong, and Z. L. Wang, Nano Lett. **7**, 1323 (2007).
[3]Y.-Y. Lin, Y.-Y. Lee, L. Chang, J.-J. Wu, and C.-W. Chen, Appl. Phys. Lett. **94**, 063308 (2009).
[4]O. Taratula, E. Galoppini, D. Wang, D. Chu, Z. Zhang, H. Chen, G. Saraf, and Y. Lu, J. Phys. Chem. B **110**, 6506 (2006).
[5]S. Kuehn, S. Friede, S. Sadofev, S. Blumstengel, F. Henneberger, and T. Elsaesser, Appl. Phys. Lett. **103**, 191909 (2013).
[6]Y. Cao, E. Galoppini, P. I. Reyes, and Y. Lu, Langmuir **29**, 7768 (2013).
[7]K. Yao, L. Chen, Y. Chen, F. Li, and P. Wang, J. Phys. Chem. C **116**, 3486 (2012).
[8]S. K. Hau, Y.-J. Cheng, H.-L. Yip, Y. Zhang, H. Ma, and A. K.-Y. Jen, ACS Appl. Mater. Interfaces **2**, 1892 (2010).
[9]X. Tian, J. Xu, and W. Xie, J. Phys. Chem. C **114**, 3973 (2010).
[10]A. Lenz, L. Selegård, F. Söderlind, A. Larsson, P. O. Holtz, K. Uvdal, L. Ojamäe, and P.-O. Käll, J. Phys. Chem. C **113**, 17332 (2009).
[11]O. Taratula, E. Galoppini, R. Mendelsohn, P. I. Reyes, Z. Zhang, Z. Duan, J. Zhong, and Y. Lu, Langmuir **25**, 2107 (2009).
[12]A. Gupta, B. C. Kim, E. Edwards, C. Brantley, and P. Ruffin, Adv. Mater. Res. **567**, 228 (2012).
[13]Y. K. Gao, F. Traeger, O. Shekhah, H. Idriss, and C. Wöll, J. Colloid Interface Sci. **338**, 16 (2009).
[14]G. Jayalakshmi, K. Saravanan, and T. Balasubramanian, J. Lumin. **140**, 21 (2013).
[15]G. Jayalakshmi and T. Balasubramanian, J. Mater. Sci.-Mater. Electron. **24**, 2928 (2013).
[16]K. Ogata, K. Koike, S. Sasa, M. Inoue, and M. Yano, J. Vac. Sci. Technol. B **27**, 1834 (2009).
[17]C. G. Allen, D. J. Baker, J. M. Albin, H. E. Oertli, D. T. Gillaspie, D. C. Olson, T. E. Furtak, and R. T. Collins, Langmuir **24**, 13393 (2008).
[18]J. A. Soares, J. E. Whitten, D. W. Oblas, and D. M. Steeves, Langmuir **24**, 371 (2008).
[19]C. L. Perkins, J. Phys. Chem. C **113**, 18276 (2009).
[20]K. Ogata, K. Koike, S. Sasa, M. Inoue, and M. Yano, Appl. Surf. Sci. **241**, 146 (2005).
[21]P. W. Sadik, S. J. Pearton, D. Norton, E. Lambers, and F. Ren, J. Appl. Phys. **101**, 104514 (2007).
[22]J. Singh, J. Im, E. J. Watters, J. E. Whitten, J. W. Soares, and D. M. Steeves, Surf. Sci. **609**, 183 (2013).
[23]C. Hariharan, Appl. Catal. A: Gen. **304**, 55 (2006).
[24]E. Galoppini, J. Rochford, H. Chen, G. Saraf, Y. Lu, A. Hagfeldt, and G. Boschloo, J. Phys. Chem. B **110**, 16159 (2006).
[25]J. Chen, R. E. Ruther, Y. Tan, L. M. Bishop, and R. J. Hamers, Langmuir **28**, 10437 (2012).
[26]H. Yip, S. K. Hau, N. S. Baek, H. Ma, and A. K. Y. Jen, Adv. Mater. **20**, 2376 (2008).
[27]N. H. Moreira, A. L. Rosa, and T. Frauenheim, Appl. Phys. Lett. **94**, 193109 (2009).
[28]T. L. Bahers, T. Pauporté, F. Labat, and I. Ciofini, Langmuir **27**, 3442 (2011).
[29]N. H. Moreira, A. Dominguez, T. Frauenheim, and A. L. da Rosa, Phys. Chem. Chem. Phys. **14**, 15445 (2012).
[30]T. L. Bahers, T. Pauporté, F. Odobel, F. Labat, and I. Ciofini, Int. J. Quantum Chemistry **112**, 2062 (2012).
[31]A. Calzolari, A. Ruini, and A. Catellani, J. Am. Chem. Soc. **133**, 5893 (2011).
[32]S. Blumstengel, H. Glowatzki, S. Sadofev, N. Koch, S. Kowarik, J. Rabe, and F. Henneberger, Phys. Chem. Chem. Phys. **12**, 11642 (2010).
[33]A. L. Briseno, T. W. Holcombe, A. I. Boukai, E. C. Garnett, S. W. Shelton, J. J. M. Fréchet, and P. Yang, Nano Lett. **10**, 334 (2010).
[34]A. Neubauer, J. M. Szarko, A. F. Bartelt, R. Eichberger, and T. Hannappel, J. Phys. Chem. C **115**, 5683 (2011).
[35]A. Amat and F. D. Angelis, Phys. Chem. Chem. Phys. **14**, 10662 (2012).
[36]C. Caddeo, G. Malloci, G.-M. Rignanese, L. Colombo, and A. Mattoni, J. Phys. Chem. C **116**, 8174 (2012).
[37]P. Ruankham, L. Macaraig, T. Sagawa, H. Nazakumi, and S. Yoshikawa, J. Phys. Chem. C **115**, 23809 (2011).
[38]A. Dominguez, N. H. Moreira, G. Dolgonos, A. L. Rosa, and T. Frauenheim, J. Phys. Chem. C **115**, 6491 (2011).
[39]X. Q. Shi, H. Xu, M. V. Hove, N. Moreira, A. Rosa, and T. Frauenheim, Surf. Sci. **606**, 289 (2012).
[40]J. Perdew, K. Burke, and M. Ernzerhof, Phys. Rev. Lett. **77**, 3865 (1996).
[41]J. P. Perdew, K. Burke, and M. Ernzerhof, Phys. Rev. Lett. **78**, 1396 (1997).

[42]L. Ley, R. A. Pollak, F. R. McFeely, S. P. Kowalczyk, and D. A. Shirley, Phys. Rev. B **9**, 600 (1974).
[43]M. Shishkin and G. Kresse, Phys. Rev. B **75**, 235102 (2007).
[44]J. Paier, M. Marsman, K. Hummer, G. Kresse, I. C. Gerber, and J. G. Ángyán, J. Chem. Phys. **124**, 154709 (2006).
[45]C. Adamo and V. Barone, J. Chem. Phys. **110**, 6158 (1999).
[46]M. Ernzerhof and G. E. Scuseria, J. Chem. Phys. **110**, 5029 (1999).
[47]G. Kresse and J. Hafner, Phys. Rev. B **47**, 558 (1993).
[48]G. Kresse and J. Hafner, Phys. Rev. B **49**, 14251 (1994).
[49]G. Kresse and J. Furthmüller, Comput. Mater. Sci. **6**, 15 (1996).
[50]G. Kresse and J. Furthmüller, Phys. Rev. B **54**, 11169 (1996).
[51]P. E. Blöchl, Phys. Rev. B **50**, 17953 (1994).
[52]G. Kresse and D. Joubert, Phys. Rev. B **59**, 1758 (1999).
[53]H. J. Monkhorst and J. D. Pack, Phys. Rev. B **13**, 5188 (1976).
[54]J. D. Pack and H. J. Monkhorst, Phys. Rev. B **16**, 1748 (1977).
[55]*Semiconductors—Basic Data*, 2nd ed., edited by O. Madelung (Springer, 1996).
[56]A. Carvalho, A. Alkauskas, A. Pasquarello, A. K. Tagantsev, and N. Setter, Phys. Rev. B **80**, 195205 (2009).
[57]J. Wróbel, K. J. Kurzydłowski, K. Hummer, G. Kresse, and J. Piechota, Phys. Rev. B **80**, 155124 (2009).
[58]A. Dominguez, S. grosse Holthaus, S. Koppen, T. Frauenheim, and A. L. da Rosa, Phys. Chem. Chem. Phys. **16**, 8509 (2014).
[59]M. C. Toroker, D. K. Kanan, N. Alidoust, L. Y. Isseroff, P. Liao, and E. A. Carter, Phys. Chem. Chem. Phys. **13**, 16644 (2011).
[60]P. Umari, L. Giacomazzi, F. D. Angelis, M. Pastore, and S. Baroni, J. Chem. Phys. **139**, 014709 (2013).
[61]K. Noori and F. Giustino, Adv. Funct. Mater. **22**, 5089 (2012).
[62]J. Kang, S. Tongay, J. Zhou, J. Li, and J. Wu, Appl. Phys. Lett. **102**, 012111(2013).
[63]W. Fan, H. Xu, A. L. Rosa, T. Frauenheim, and R. Q. Zhang, Phys. Rev. B **76**, 073302 (2007).
[64]A. Miranda, X. Cartoixa, E. Canadell, and R. Rurali, Nanoscale Research Letters **7**, 308 (2012).
[65]J. W. Spalenka, P. Gopalan, H. E. Katz, and P. G. Evans, Appl. Phys. Lett. **102**, 041602 (2013).
[66]G. Jayalakshmi, N. Gopalakrishnan, and T. Balasubramanian, J. Alloys Compd. **551**, 667 (2013).